

OCCULTATION OBSERVATION TO PROBE THE TURBULENCE SCALE SIZE IN THE PLASMA TAIL OF COMET SCHWASSMANN-WACHMANN 3-B

NIRUPAM ROY,¹ P. K. MANOHARAN,² AND PAVAN CHAKRABORTY³

Received 2007 July 6; accepted 2007 August 24; published 2007 September 25

ABSTRACT

We present the occultation observation of compact radio source B0019–000 through the plasma tail of comet Schwassmann-Wachmann 3-B. The observation was made with the Ooty Radio Telescope at 326.5 MHz on 2006 May 26, when the plasma tail of the comet was in front of this source. The scintillation was found to be increased significantly for the target source compared to that of a control source. The intensity fluctuation power spectra show both steepening at high spatial scales and excess power at low spatial scales. This observation can be attributed to the turbulence in the comet plasma tail. A two-regime plasma turbulence can explain the time-evolution of the power spectrum during the occultation observation.

Subject headings: comets: general — comets: individual (73P/Schwassmann-Wachmann 3-B) — interplanetary medium — occultations — turbulence

1. INTRODUCTION

The interplanetary scintillation (IPS) technique is a useful, convenient, remote-sensing method to probe the solar wind (Hewish et al. 1964; Manoharan 1993). It exploits the scattering of radio waves from a compact radio source by the density irregularities in the solar wind and provides information on the speed and turbulence spectrum of the solar wind plasma at the region of closest solar offset of the line of sight to the radio source (e.g., Manoharan 1993). When a comet plasma tail intersects the radio path, the electron density irregularities associated with the comet can cause an enhancement in the level of scintillation. Several attempts have been made to estimate the turbulence associated with the cometary plasma by observing the occultation of the radio source by the tail of the comet (Ananthakrishnan et al. 1975, 1987; Alurkar et al. 1986, 1989; Slee et al. 1987; Hajivassiliou & Duffett-Smith 1987). However, in order to confirm the effect of the cometary plasma as well as to assess the contribution to the level of turbulence imposed by any solar wind transients or disturbances, it is essential to simultaneously monitor a region just outside the tail of the comet during such observations.

Ananthakrishnan et al. (1987) reported a significant increase in the plasma turbulence as the tail of comet Halley approached a radio source. But, a rather similar enhancement in scintillation was also observed toward control sources, which were located outside the comet tail (Ananthakrishnan et al. 1987). This emphasized the need for near-simultaneous monitoring of IPS through the tail of the comet as well as a region outside the comet tail. This study attributed an insignificant increase of turbulence associated with the cometary plasma. In a later work, Slee et al. (1990) adopted the idea of near-simultaneous observation of control source during cometary occultation observation and reported a significant increase of the scintillation of the target source compared to that of the control source. In this Letter we report the occultation of the compact radio source B0019–000 by the plasma tail of comet Schwassmann-Wachmann 3-B. The results are substantiated by the observations of

the IPS of a control source outside the tail. Systematic changes observed in the IPS spectra as the source approached the comet tail suggest a steeper turbulence spectrum for the cometary plasma at scales >500 km and excessive turbulence at the small-scale part (i.e., <50 km) of the spectrum. Below, in § 2, we give the details of our observations and the results. We compare the results with previously reported results and discuss the actual astrophysical implication of the results in § 3. Finally, we summarize and present our conclusions in § 4.

2. OBSERVATIONS AND RESULTS

The comet Schwassmann-Wachmann 3 (also known as 73P/Schwassmann-Wachmann) is a periodic comet. This Jupiter-family comet passed within ~ 0.1 AU of the Earth around the middle of 2006. It is to be noted that the comet was going through breaking and disintegration (Boehnhardt & Kaufl 1995; Crovisier et al. 1996; Boehnhardt et al. 2002), which would likely to increase the level of turbulence. The occultation observation reported here was therefore aimed at estimating the turbulence spectrum of density irregularities and associated scale sizes of the cometary plasma.

Compact sources lying close to the path of the comet were chosen from the Molonglo Catalogue (Large et al. 1981). On 2006 May 26, one of the fragments (labeled 73P-B, the second brightest fragment at the time of observation) aligned along the line of sight to the radio source B0019–000, which has a compact component (~ 50 mas) containing $>75\%$ of the total flux density, $S_{408} = 2.99 \pm 0.14$ Jy. The line of sight along the radio source B0019–073 ($S_{408} = 1.83 \pm 0.07$ Jy) was monitored as the control region. The systematic monitoring of these sources on the day of occultation as well as for the next two consecutive days provide the spectrum of the density irregularities and dominant scale sizes of the cometary plasma. This Target of Opportunity observation was carried out using the Ooty Radio Telescope (ORT) at the Radio Astronomy Centre, Ooty (Swarup et al. 1971). The ORT, an equatorially mounted parabolic cylindrical antenna, is 530 m long in the north-south direction and 30 m wide in east-west direction. It operates at 326.5 MHz and can effectively probe solar wind in the heliocentric distance range of 0.05–1.0 AU.

On 2006 May 26–28, both the target source (B0019–000) and the control source (B0019–073) were observed. The coordinates and flux densities of these sources are given in Table 1. The orbital

¹ NCRA-TIFR, Post Bag 3, Ganeshkhind, Pune 411 007, India; nirupam@ncra.tifr.res.in.

² Radio Astronomy Centre, NCRA-TIFR, P.O. Box 8, Udhagamandalam 643 001, India; mano@ncra.tifr.res.in.

³ Indian Institute of Information Technology, Deoghat, Jhalwa, Allahabad 211 012, India; pavan@iita.ac.in.

TABLE 1
RADIO SOURCES PARAMETERS

IAU NAME		ECLIPTIC COORDINATES (J2000.0) (deg)		S_{408}^a (Jy)
B1950.0	J2000.0			
0019-000	0022+002	5.245, -1.998		2.99 ± 0.14
0019-073	0022-070	2.320, -8.685		1.83 ± 0.07

^a From Molonglo Reference Catalogue (Large et al. 1981).

parameters of the comet Schwassmann-Wachmann 3-B are summarized in Table 2. Figure 1 shows the position of the nucleus of the comet on 2006 May 26–28 with respect to the position of both the target and control sources, projected on the plane of the sky. Figure 2 displays the comet trajectory on 2006 May 26 overplotted on the 1.4 GHz image of the field centered at the target source B0019–000 taken from the NRAO VLA Sky Survey (NVSS; Condon et al. 1998). The positions of the comet on these days are taken from the online high-precision ephemerides provided by Jet Propulsion Laboratory (JPL) solar system dynamics group. The target source was observed during occultation on 2006 May 26 from 0713 to 0804 UT (when the target hour angle reached the west limit of the ORT) at 326.5 MHz with a total bandwidth of 4.0 MHz and a time resolution of 20 ms. During this span, the control source was observed for a short period to understand the solar wind characteristics and to distinguish between any changes caused by the turbulence in the tail of the comet and the solar wind. Note that the control source is sufficiently close to the target source. So, these two lines of sight are expected to have similar solar wind characteristics. A nearby cold region of the sky was also observed to get the “off-source” reference. Both the target and the control sources were observed again on 2006 May 27 and 28.

A detailed account of the IPS observation using the ORT and data analysis procedure is given in Manoharan (2003). In brief, the Fourier transformation and spectrum computation from the recorded intensity scintillation measurements are performed to get the power spectrum of the intensity fluctuations to bring out the statistical properties of the intervening medium. A 2048-point fast Fourier transformation yields a frequency resolution of ≈ 0.025 Hz. The spectrum is corrected for the off-source noise and the averaging of the adjacent spectral points gives a uniform noise up to the cutoff frequency (where the power drops to noise level). The area under the power spectrum is the measure of the scintillation index. Since the present measurements are made in the weak scattering region, the shape of the spectrum and the scintillation index are directly related to the turbulence spectrum of the intervening plasma and the level of plasma turbulence, respectively (Manoharan 1993).

As illustrated in Figure 3, significant changes are evident in the shape of the power spectrum as the comet nucleus approached the line of sight to the radio source. The time of

TABLE 2
COMET 73P/SCHWASSMANN-WACHMANN 3-B PARAMETERS

Date at 0800 UT	Nuclear Ecliptic Coordinates (deg)	Heliocentric Distance (AU)	Topocentric Distance (AU)	Elongation Leading (deg)
May 26	251.15, -0.25	0.957	0.1216	59.62
May 27	252.48, -0.52	0.955	0.1287	59.60
May 28	253.82, -0.79	0.952	0.1360	59.70

NOTE.—From JPL solar system dynamics group.

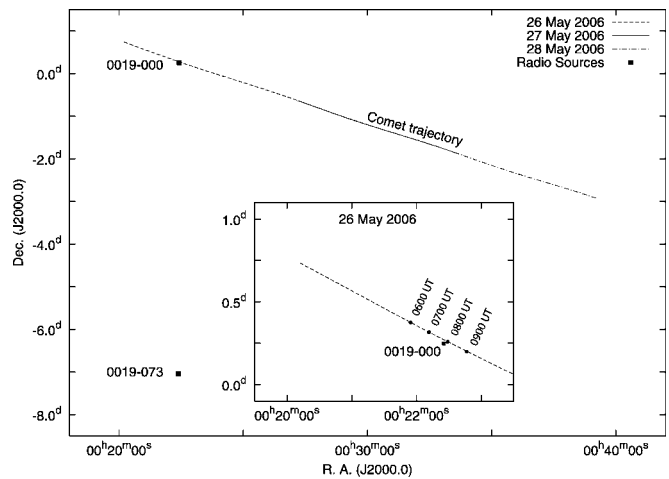


FIG. 1.—Path of the comet with respect to the radio sources (both the target and the control source). The position of the comet nucleus on 2006 May 26–28 is plotted. Part of the trajectory on 2006 May 26 is shown in the inset, where the positions close to the time of observation are marked.

observation (in UT) for each spectrum is given on the top right of each panel. The details of the implication of the power spectrum shape and the interpretation of scale size from IPS spectral variation are described in Manoharan et al. (1994, 2000). Panels *a–c* in Figure 3 show the change of the power spectra during occultation on 2006 May 26. Panels *d* and *e* are the power spectra from the follow-up observations on 2006 May 27 and 28, respectively. The power spectra for the control source taken on May 26 (near simultaneous to occultation observation), 27, and 28 are shown in panels *i–h*, respectively. The spectrum toward the source obtained from the first half of the observation (0713–0740 UT) on May 26 has no significant change. But spectra from the later part of the observation

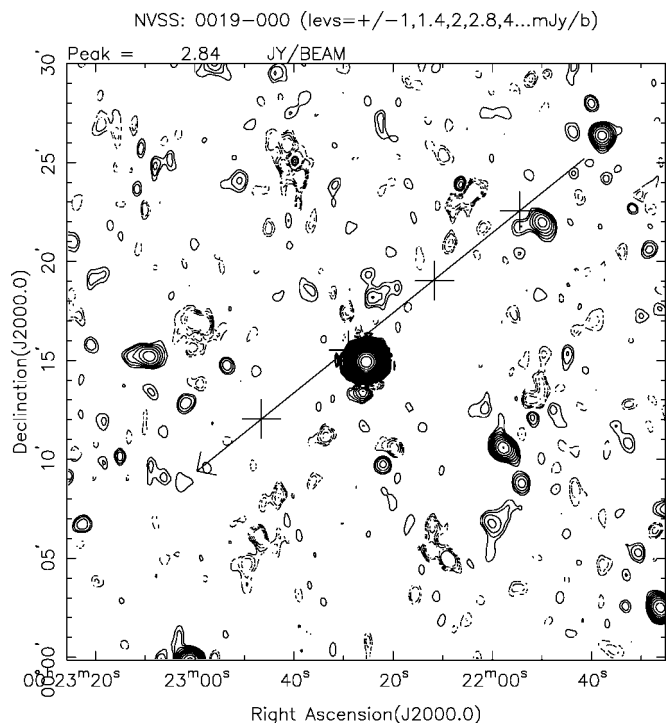


FIG. 2.—NVSS *L*-band image of the field centered at the target source 0019–000. Part of the trajectory on 2006 May 26 is overplotted with the positions at 0600, 0700, 0800, and 0900 UT (top right to bottom left) marked with crosses.

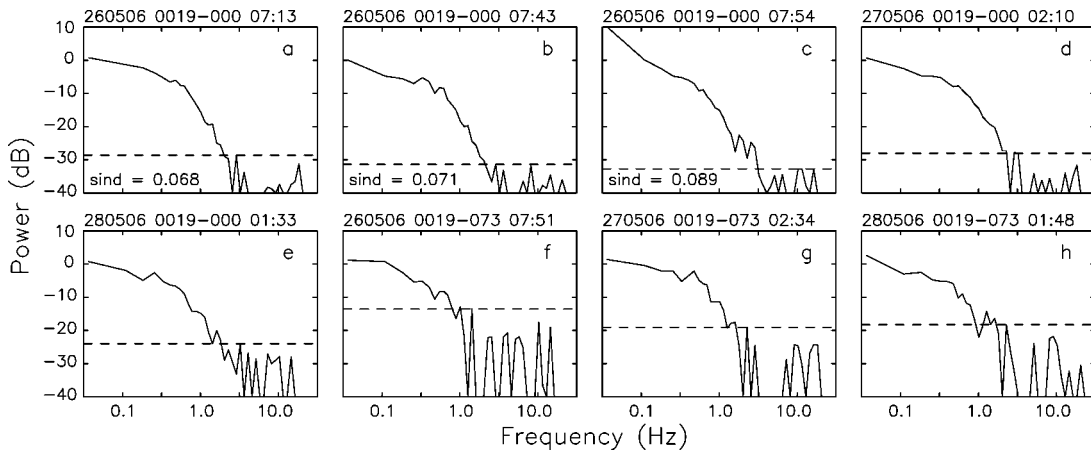


FIG. 3.—Power spectra of the intensity fluctuation. The horizontal axis is the spectral frequency (Hz) and the vertical axis is power (dB). Date, source name, and the time of observation (UT) are given at the top of each panel. The dashed lines indicate the noise power level. Note the steepening of the spectrum at high spatial scales (panels *b* and *c*) and significant excess power at low spatial scales (panel *c*) compared to the rest of the spectra from follow-up and control observations (see § 2 for details).

(0743–0804 UT) shows steepening at lower spatial frequency. The scale size $a = v/(2\pi f)$, where f is the temporal frequency and v is the solar wind speed. Considering a typical solar wind speed of $\sim 400 \text{ km s}^{-1}$, this translates to spatial scales of $>500 \text{ km}$. Excess power is also seen at low spatial scales ($<50 \text{ km}$) on the spectrum obtained from the end part of the observation (0754–0804 UT). The shape of the power spectra of the control observations shows normal quiet solar wind condition. The changes in the spectra during the occultation are attributed to the turbulence in the comet plasma tail.

We find that the scintillation index of the control source was normal during these observations and also during the control observations on the following days, implying normal quiet solar wind conditions. But we have noticed significant changes in the scintillation index for the target source. The scintillation index increased, in about 1 hr during the course of our observation, from 0.068 to 0.089. It is clear from the power spectra that the steepening at the high spatial scales is the dominant source of this enhancement. Here we consider the ratio of the level of the electron density spectrum Φ_{ne} to the mean squared

electron density $\langle n_e^2 \rangle$ to be a measure of plasma turbulence. For an intervening medium of effective thickness L , the scintillating flux density variance $\Delta S^2 \propto \Phi_{ne} L$. From this, we can relate the change of measured scintillation index to the physical parameters of solar wind and cometary plasma,

$$\frac{\Delta S^2}{\langle \Delta S^2 \rangle} = \frac{(\Phi_{ne}/n_e^2)_s n_{es}^2 L_s + (\Phi_{ne}/n_e^2)_c n_{ec}^2 L_c}{(\Phi_{ne}/n_e^2)_s n_{es}^2 L_s}, \quad (1)$$

where the subscripts s and c refer to solar and cometary, respectively, and $\langle \Delta S^2 \rangle$ is the estimated variance due to the solar wind on that day.

We have used the data obtained from scintillation monitoring observations from the ORT for many years toward 0019–000 to get the scintillation index as a function of heliocentric distance of the point of closest approach of the line of sight (see Manoharan [1993, 2006] for details of scintillation index variation with heliocentric distance). During our observation the average heliocentric distance was $\sim 185.5 R_\odot$. Figure 4 shows the long-time average of the scintillation index, and from this, for normal solar wind conditions, the expected scintillation index is 0.061 at $185.5 R_\odot$ for a flux density of 3.0 Jy . This corresponds to $\langle \Delta S^2 \rangle^{0.5} = 183 \text{ mJy}$. Please note that the peak scintillation index is ~ 0.8 for this source. This implies that the source is very compact ($\leq 50 \text{ mas}$) and is an ideal source for scintillation measurements. From our occultation data we can find, using equation (1), the normalized level of turbulence (Φ_{ne}/n_e^2) in the comet plasma tail compared to that in the solar wind. We assume typical values for L_s and L_c to be 10^8 and 10^5 km , respectively. Considering that the radio source line of sight probes the plasma tail about $1.4 \times 10^4 \text{ km}$ away from the nucleus and that the angular size of the coma was $\sim 3'$, the expected value of L_c is $\sim 5 \times 10^4 \text{ km}$. $L_c = 10^5 \text{ km}$ may be taken as an upper limit and, for smaller values of L_c , the corresponding value of $(\Phi_{ne}/n_e^2)_c$ will increase. Average electron number density in the cometary plasma is assumed to be $n_{ec} = 30 \text{ cm}^{-3}$ (Grard et al. 1986). Earlier reports (Alurkar et al. 1986; Slee et al. 1987; Ananthakrishnan et al. 1987) used, following Reme et al. (1986), $n_{es} = 5 \text{ cm}^{-3}$ for normal solar wind condition. We have instead taken the average value of number density to be 7 cm^{-3} computed from the 1 minute OMNI data (from the CDAWeb service of the NASA/GSFC Space Physics Data Facility) for the period of 2006 May 21–

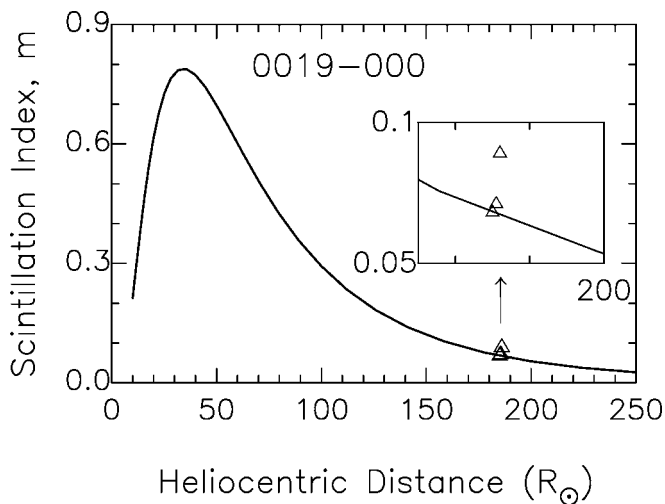


FIG. 4.—Scintillation index enhancement in occultation. The solid line represents the long-time average of the scintillation index as a function of heliocentric distance of the point of closest approach of the line of sight toward 0019–000 obtained from scintillation monitoring for many years from the ORT. The triangles are measurements during occultation. The part of the plot of our interest is magnified in the inset.

31. We summarize the result of plasma turbulence enhancement in Table 3.

3. DISCUSSION

We present the detection of a rare event of the occultation of a compact source (B0019–000) by the plasma tail of comet Schwassmann-Wachmann 3-B using scintillation observation and the power spectral analysis. It is interesting to compare the present results with the earlier reports of both detections and nondetections of enhanced scintillation. The range of values of the normalized plasma turbulence from similar observations spread over almost an order of magnitude (Alurkar et al. 1986; Slee et al. 1987, 1990; Ananthakrishnan et al. 1987) for a given set of parameters (e.g., L_c , n_{ec}). In addition to that, the turbulence level is likely to change systematically with the distance from the nucleus of the comet along the plasma tail axis. In other words, occultation observations probe the plasma at different distances from the comet nucleus and hence may reveal a variety of turbulence levels. Hence a straightforward quantitative comparison of plasma turbulence is not possible. But from earlier results, the clear trend emerges that most of the negative results can be attributed to a chance of actually probing a lower level of turbulence in the occultation events (Slee et al. 1990) for various reasons. The rest of the cases with favorable observing geometry have resulted in a positive detection. In the present study, given the possibility of enhanced level of turbulence because of the ongoing disintegration and the small offset of the line of sight from the nucleus of the comet, our result is in good agreement with this scenario.

The change of the intensity fluctuation power spectra has contributions in two distinct scales. The steepening of the spectrum at low frequency indicates scale sizes in the intervening plasma at high spatial scales and remarkable turbulence enhancement associated in this spectral region. For a typical solar wind speed of 400 km s^{-1} , it translates to linear scales of >500 km. At the later part of the observation, at the close encounter of the comet nucleus and the line of sight to the radio source, we notice the additional significant contribution in the power spectrum at the low-frequency region, which corresponds to linear scales of <50 km. It is to be noted that the IPS measurements normally show much less turbulence at these small scales. The evolution of the spectrum with time during the course of the occultation indicates that the plasma turbulence level is dominated by small-scale density irregularities closer to the tail axis. However, it is the large-scale irregularities, developed most likely due to the interaction of plasma with

TABLE 3
PARAMETERS FOR THE PLASMA TAIL ON MAY 26

Time (UT)	Flux ^a (Jy)	Scintillation Index	ΔS^b (mJy)	$\Delta S^2/(\Delta S^2)$	$(\Phi_{ne}/n_e^2)_c/(\Phi_{ne}/n_e^2)_c$
0725	3.1	0.068	210.8	1.327	17.8
0750	3.0	0.071	213.0	1.355	19.3
0800	2.7	0.089	240.3	1.724	39.4

^a Flux density measurement is limited by the ORT confusion.

^b ΔS is not limited by confusion and is much accurate.

the ambient solar wind and the evaporation process, that contribute significantly at the outer part of the tail. This shows the presence of two main regimes of turbulence in the comet plasma tail. This is found to be in agreement with the earlier reported results of Slee et al. (1987, 1990) for the cases of comet Halley and comet Wilson, where similar two-regime plasma turbulences were detected.

4. CONCLUSIONS

We have present the results from the occultation observation of a compact radio source B0019–000 at 326.5 MHz through the plasma tail of comet Schwassmann-Wachmann 3-B. We detect significant enhancement in the scintillation index and change in the intensity fluctuation power spectrum during the occultation period. The systematic study of the evolution of power spectrum clearly reveals the dominant effect of large-scale (>500 km) density fluctuations and the presence of a smaller scale (<50 km) closer to the tail axis. Since the shape of the power spectra of all the control observations show normal quiet solar wind condition, these changes at the time of occultation are attributed to the plasma tail of the comet. This clearly shows the presence of a two-regime plasma turbulence with two distinct scales of density irregularities that may arise from the interaction of solar wind with the comet plasma tail.

We thank Jayaram N. Chengalur, C. H. Ishwara-Chandra, and Rajaram Nityananda for much encouragement and many helpful comments. We are grateful to the observing staff of the ORT. One of the authors (P. C.) is thankful to IUCAA for sponsoring his research under the IUCAA visiting associateship program. We are also grateful to the anonymous referee for useful comments and for prompting us into substantially improving this paper. This research has made use of NASA's Astrophysics Data System, the JPL Solar System Dynamics Web site, the CDAWeb service of the NASA/GSFC Space Physics Data Facility, and the NVSS data products.

REFERENCES

- Alurkar, S. K., Bhonsle, R. V., & Sharma, A. K. 1986, *Nature*, 322, 439
 Alurkar, S. K., Sharma, A. K., Janardhan, P., Bhonsle, R. V., Ananthakrishnan, S., Manoharan, P. A., & Venugopal, V. R. 1989, *Nature*, 338, 211
 Ananthakrishnan, S., Manoharan, P. K., & Venugopal, V. R. 1987, *Nature*, 329, 698
 Ananthakrishnan, S., Rao, A. P., & Bhandari, S. M. 1975, *Ap&SS*, 37, 275
 Boehnhardt, H., Holdstock, S., Hainaut, O., Tozzi, G. P., Benetti, S., & Licandro, J. 2002, *Earth Moon Planets*, 90, 131
 Boehnhardt, H., & Kaufl, H. U. 1995, *IAU Circ.* 6274
 Condon, J. J., Cotton, W. D., Greisen, E. W., Yin, Q. F., Perley, R. A., Taylor, G. B., & Broderick, J. J. 1998, *AJ*, 115, 1693
 Crovisier, J., Bockelée-Morvan, D., Gerard, E., Rauer, H., Biver, N., Colom, P., & Jorda, L. 1996, *A&A*, 310, L17
 Grard, R., Pedersen, A., Trotignon, J. G., Beghin, C., Mogilevsky, M., Mikhailov, Y., Molchanov, O., & Formisano, V. 1986, *Nature*, 321, 290
 Hajivassiliou, C. A., & Duffett-Smith, P. J. 1987, *MNRAS*, 229, 485
 Hewish, A., Scott, P. F., & Wills, D. 1964, *Nature*, 203, 1214
 Large, M. I., Mills, B. Y., Little, A. G., Crawford, D. F., & Sutton, J. M. 1981, *MNRAS*, 194, 693
 Manoharan, P. K. 1993, *Sol. Phys.*, 148, 153
 ———. 2003, in *Lectures on Solar Physics*, ed. H. M. Antia et al. (Berlin: Springer), 299
 ———. 2006, *Sol. Phys.*, 235, 345
 Manoharan, P. K., Kojima, M., Gopalswamy, N., Kondo, T., & Smith, Z. 2000, *ApJ*, 530, 1061
 Manoharan, P. K., Kojima, M., & Misawa, H. 1994, *J. Geophys. Res.*, 99, 23411
 Reme, H., et al. 1986, *Nature*, 321, 349
 Slee, O. B., Bobra, A. D., Waldron, D., & Lim, J. 1990, *Australian J. Phys.*, 43, 801
 Slee, O. B., McConnell, D., Lim, J., & Bobra, A. D. 1987, *Nature*, 325, 699
 Swarup, G., et al. 1971, *Nature*, 230, 185